DOI: 10.6060/mhc214017a

meso-Expanded Co^{III}triarylcorroles with One to Three Nitrophenyl Moieties: Synthesis, Characterization and Tunable Electrochemical Catalysis

Isaac Kwaku Attatsi,[#] Yuanyuan Qiu,[#] Weihua Zhu, Long Zhao,[@2] and Xu Liang[@1]

School of Chemistry and Chemical Engineering, Jiangsu University, Zhenjiang 212013, P. R. China
[@1]*Corresponding author e-mail: liangxu@ujs.edu.cn*
[@2]*Corresponding author e-mail: longzhao@ujs.edu.cn*
[#] *These authors contributed equally*

To find the effect of electron distribution on the molecules on electrocatalysis performance, we have rationally synthesized three cobalt corrole molecules with different numbers of nitrophenyl groups at the periphery. The electron withdrawing nitrophenyl substituents alter the electron localization of the molecules, thus leading to variation in spectroscopy and electrochemistry of the cobalt corroles. The hydrogen evolution reaction (HER), oxygen evolution reaction (OER) and oxygen reduction reaction have been investigated using different solutions, showing that Cor-N1 is best for HER while Cor-N2 is most suitable for OER.

Keywords: Co^{III}corroles, electronic structure, spectroscopy, electrocatalysis.

мезо-Расширенные Co^{III}триарилкорролы с нитрофенильными фрагментами: синтез, характеристика и настраиваемый электрохимический катализ

И. К. Аттаци,[#] Ю. Кью,[#] В. Жу, Л. Жао,[@1] Сюй Лян[@2]

Школа химии и химического машиностроения, Университет Цзянсу, Чжэньцзян 212013, КНР
[@1] *longzhao@ujs.edu.cn*
[@2] *liangxu@ujs.edu.cn*
[#] *Эти авторы внесли одинаковый вклад*

Для выяснения влияния электронного распределения на эффективность электрокатализа синтезированы три Co^{III}комплекса коррола с разным числом нитрофенильных групп на периферии. Электроноакцепторные нитрофенильные заместители изменяют электронную локализацию, что приводит к изменению спектральных свойств и электрохимии полученных комплексов. Реакция выделения водорода (HER), реакция выделения кислорода (OER) и реакция восстановления кислорода были исследованы с использованием различных растворов; показано, что Cor-N1 является наиболее подходящим для HER, тогда как Cor-N2 – для OER.

Ключевые слова: Co^{III}корролы, электронное строение, спектроскопия, электрокатализ.

Introduction

Hydrogen evolution reaction (HER), oxygen evolution reaction (OER) and oxygen reduction reaction (ORR) are very important reactions for understanding the gas-solid interface charge transfer mechanism and application in fuel cells, water splitting and bio-fuel reactions.[1–3] Typically, platinum-based catalysts are widely used by modify-

ing with some other functional dopants for the three types of reactions since the natural optimized surface energy of adsorption and desorption of Pt to H^+, O^{2-} and OH^-.[4–6] The main concern of using noble metal is the high cost restraining the industrialization.[7–9] Exploiting cheap materials, especially those materials that are easy to tailor would be quite an operational approach to fulfill the commercial requirement for HER, OER and ORR catalyzing.[10–13] Corrole derivatives, especially metal coordinated corroles, are very promising for the aforementioned reactions mainly due to their ease of structure modification and stubborner than porphyrins for oxidations.[14–16] Previous reports have shown that cobalt corroles are effective in HER, have much lower overpotential for OER and competitive oxidation potentials for oxygen compared to other macrocyclic compounds.[17] These findings though indicate the utility of the corrole macrocycles in electrochemistry, the mechanism of these molecules regarding the molecular structure effect has not been deeply explored.[18–20] Structure of corrole complexes is generally modified from the following aspects. The first method is tuning the substituents of the corrole cycle therefore altering the symmetry of the molecules and/or the energy levels of the materials.[2,21–24] For instance, we have synthesized Co^{III}corroles with different peripheral *meso*-substituted groups and their electrochemical measurement showed the differences in energy levels depend on substituents. The second commonly employed approach is the change of central metal, for example Cu(II), Zn(II), Ni(II),[25–27] *etc.* A successful ORR catalyst has been reported based on the central metal cation of the corrole complex. Besides, attaching ligands to the center metal of corrole complex has also proved to be helpful for enhancing the stability or performance of OER.[22,23,28–30] A series of Co^{III}corroles has been reported by our group recently using corrole cycle as the skeleton, cobalt ion as the coordinated metal to enhance the oxygen reduction property and PPh_3 as coordinated ligands to the metal core to stabilize the molecule at oxidized circumstance.[21,31] The electrochemical, DFT and catalysis measurements demonstrated the feasibility of the type of molecules in HER, OER and ORR performance.[24,32] In this work, the structure of the molecules was modified with different number of electron-withdrawing groups to vary the electron density on the skeleton and the effects of these substituents on HER, OER and ORR performance were investigated.

Experimental

All reagents and solvents used were of reagent grade and were used as received unless noted otherwise. ^{1}H NMR spectra were recorded on a Bruker AVANCE 400 spectrometer (400.03 MHz). Residual solvent peaks were used to provide internal references (δ = 7.26 ppm for $CDCl_3$). Fourier transform infrared spectrum (FT-IR) was taken using KBr pellet method on Nicolet Nexus 470 FT-IR spectrophotometer from Thermo Electron Corporation. Cyclic voltammetry (CV) was carried out on a Chi-730D electrochemistry station with a three-electrode cell. A glassy carbon disk, a platinum wire and an Ag/AgCl electrode were used as the working, counter and reference electrodes, respectively. An inert nitrogen atmosphere was introduced during all of the electrochemical measurements, which were carried out at room temperature. The UV and visible regions of the electronic absorption spectra were recorded with an HP 8453A diode array spectrophotometer.

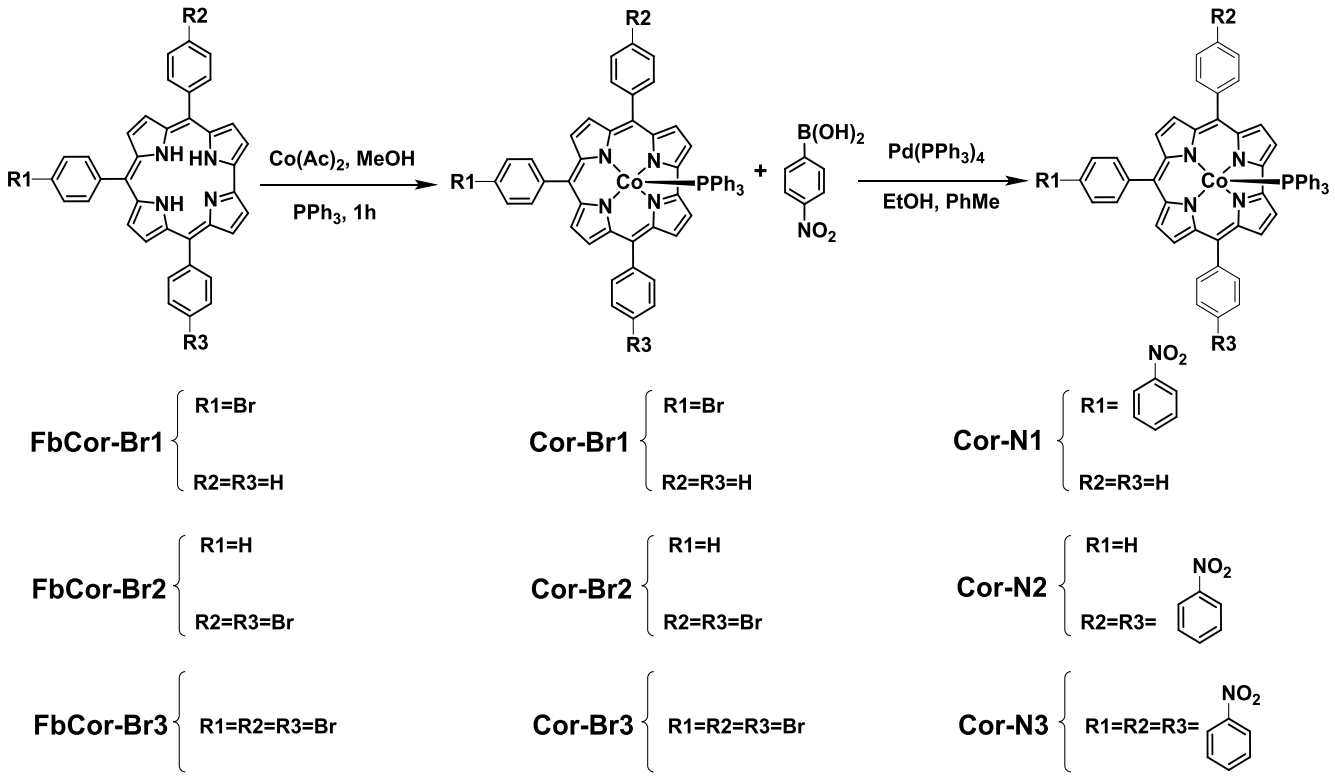

Scheme 1. General synthetic route of the investigated compounds.

Preparation of modified electrodes. 1.0 mg of rGO was mixed with 1 mL of isopropyl alcohol containing 0.2% nafion and the mixture was sonicated in an ultrasonic bath for 30 min to produce a homogeneous mixture of concentration 1 mg/mL. The surface of the glassy carbon electrode (GCE) was polished with 0.05 μm alumina and rinsed with doubly distilled water in the ultrasonic bath to remove any adhered Al_2O_3 particles. The electrodes were rinsed with ethanol and dried under room temperature for *ca.* 5 min. Three μL of the rGO/isopropyl alcohol/nafion suspensions were dropped on the surface of the GC electrode and allowed to dry at room temperature. 10 μL aliquots of 0.2 mM CH_2Cl_2 solutions of **Cor-N1-N3** were added dropwise to the rGO/nafion-coated electrodes and dried at room temperature for 1 h. The electrodes were stored in MilliQ water in the dark.

*General procedure for synthesis of **Cor-N1-3***. Co^{III}corrole **Cor-Br1-3** (0.1 mmol, 0.092g), *p*-nitrobenzoboronic acid (0.5 mmol, 0.061 g, 5.0 eq), $Pd(PPh_3)_4$ (10 μmol, 0.012 g), NaOH (0.25 mmol, 0.01 g) were mixed in 50 mL solution (30 mL toluene, 10 mL ethanol and 10 mL water), and then stirred and heated at 85 °C for 4 h under N_2. After removal of the solvents, purification was achieved through silica gel column (CH_2Cl_2 : hexane = 1:2; v:v) and bio-beads column ($CHCl_3$) to give the investigated compounds.

Co^{III}*PPh$_3$-10-(p-nitrophenyl)-5,15-diphenylcorrole* (***Cor-N1***). Yield: 10.4% (0.011 g). MALDI-TOF: *m/z* = 703.13 (Calcd. $[M]^+$ = 703.65). IR (KBr) *ν* cm^{-1}: 3440 (s), 3057 (w), 2924 (w), 2357 (w), 1596 (s), 1515 (s), 1435 (m), 1342 (vs), 1319 (m), 1110 (w), 1089 (w), 1053 (s), 1015 (m), 985 (m), 853 (w), 812 (w), 787 (w), 747 (m), 715(m), 694 (s), 522 (s). ^{1}H NMR (400 MHz, $CDCl_3$) δ_H ppm: 8.64 (2H, dd, J_1 = 9.9 Hz, J_2 = 5.2 Hz), 8.44~8.33 (4H, dt, J_1 = 10.8 Hz, J_2 = 4.7 Hz), 8.19~8.02 (6H, ddd, J_1 = 13.7 Hz, J_2 = 9.7 Hz, J_3 = 4.5 Hz), 8.01~7.92 (2H, m), 7.87 (1H, d, J = 8.3 Hz), 7.81 (1H, t, J = 7.1 Hz), 7.73~7.52 (8H, dd, J_1 = 32.6 Hz, J_2 = 12.6 Hz), 7.48 (1H, d, J = 7.3 Hz), 7.37 (1H, d, J = 7.8 Hz), 7.07 (3H, t, J = 7.0 Hz), 6.72 (6H, t, J = 6.7 Hz), 4.72 (6H, dd, J_1 = 10.0 Hz, J_2 = 8.4 Hz).

Co^{III}*PPh$_3$-5,15-di(p-nitrophenyl)-10-phenylcorrole* (***Cor-N2***). Yield: 12.9% (0.014 g). MALDI-TOF: *m/z* = 824.17 (Calcd. $[M]^+$ = 824.74). IR (KBr) *ν* cm^{-1}: 3452 (m), 3057 (w), 2923 (w), 2851 (w), 2367 (w), 1595 (s), 1557 (w), 1515 (vs), 1483 (m), 1435 (m), 1341 (vs), 1319 (m), 1226 (w), 1177(w), 1110 (w), 1089 (w), 1053 (s), 1015 (m), 985 (m), 853 (s), 816 (m), 787 (w), 754 (m), 732 (w), 715(m), 694 (s), 521 (s). ^{1}H NMR (400 MHz, $CDCl_3$) δ_H ppm: 8.68 (2H, dd, J_1 = 9.8 Hz, J_2 = 5.1 Hz), 8.47~8.35 (6H, dt, J_1 = 6.8 Hz, J_2 = 4.4 Hz), 8.23~8.14 (3H, dd, J_1 = 10.0 Hz, J_2 = 4.7 Hz),8.13~8.05 (3H, m), 8.04~7.92 (4H, m), 7.87 (3H, d, J = 7.0 Hz), 7.81 (1H, d, J = 8.2 Hz), 7.74~7.53 (5H, m), 7.51~7.44 (1H, d, J = 7.3 Hz), 7.37 (1H, d, J = 7.4 Hz), 7.08 (3H, t, J = 7.2 Hz), 6.72 (6H, td, J_1 = 8.0 Hz, J_2 = 2.0 Hz), 4.71 (6H, dd, J_1 = 10.4 Hz, J_2 = 7.9 Hz).

Co^{III}*PPh$_3$-5,10,15-tri(p-nitrophenyl)corrole* (***Cor-N3***). Yield: 6.6% (0.008 g). MALDI-TOF: *m/z* = 945.44 (Calcd. $[M]^+$ = 945.84). IR (KBr) *ν* cm^{-1}: 3442 (m), 3055 (w), 2924 (w), 2852(w), 2359 (w), 1718 (m), 1595 (s), 1515 (vs), 1434 (m), 1391 (w), 1342 (vs), 1261 (m), 1178(w), 1109 (w), 1089 (w), 1053 (m), 1015 (m), 985 (m), 853 (s), 815 (s), 787 (w), 753 (m), 730 (w), 714(w), 694 (s), 521 (s). ^{1}H NMR (400 MHz, $CDCl_3$) δ_H ppm: 8.70 (2H, dd, J_1 = 6.2 Hz, J_2 = 3.5 Hz), 8.49~8.39 (6H, ddd, J_1 = 11.3 Hz, J_2 = 6.8 Hz, J_3 = 2.9 Hz), 8.38~8.31 (2H, dd, J_1 = 11.7 Hz, J_2 = 6.8 Hz), 8.27~8.17 (3H, m), 8.16~8.08 (3H, dd, J_1 = 11.6 Hz, J_2 = 4.6 Hz), 8.04 (1H, d, J = 4.2 Hz), 8.00~8.93 (4H, dd, J_1 = 8.7 Hz, J_2 = 2.7 Hz), 7.91~7.86 (3H, d, J = 6.6 Hz), 7.83 (2H, t, J = 6.7 Hz), 7.79~7.63 (5H, m), 7.48 (1H, d, J = 7.7 Hz),7.08 (3H, t, J = 7.4 Hz), 6.72(6H, td, J_1 = 8.1 Hz, J_2 = 2.4 Hz), 4.69 (6H, dd, J_1 = 10.8 Hz, J_2 = 8.3Hz).

Results and Discussion

The electronic structure of **Cor N1-3** was investigated in CH_2Cl_2. The UV-visible absorption spectra observed for our compounds are similar to previously reported H_3-5,10,15-triphenylcorrole[33] (Figure 1). When number of nitrophenyl groups at the periphery is increased from 2 to 3, negligible changes were observed at both the Soret and the Q-band absorptions that indicates the minor influence of *meso*-substituents on the HOMO–LUMO gaps. In order to gain insight into the influence of the electronic structure, cyclic voltammetry (CV) was employed to characterize the oxidation as well as the reduction properties of the investigated molecules in solution as shown in Figure 2.

In the positive region two oxidation peaks appear for all molecules, which is consistent with the reported similar structures.[2,21,24] **Cor-N2** and **Cor-N3** show similar peak potentials for both oxidation reactions, whilst **Cor-N1** with the one nitrophenyl group displays slightly more positive oxidation potentials at 0.93 V and 1.44 V. It is contrary to the findings of some *meso*-substituted Co^{III}corroles reported previously, where we explained that the decrease in the electron density on π-conjugation system of corrole ligand is caused by attaching electron withdrawing substituents leading to significantly easier reduction and more difficult oxidation. The negative scan shows three peaks for all the molecules on the forward sweep but four peaks on the reverse sweep. A cleavage of the second reduction reaction may be assigned to the redox of Co^{III}/Co^{II} at the potential window of -0.7 V to -1.4 V. **Cor-N2** shows the lowest first reduction peak at -0.51 V as compared to the other two analogues **Cor-N3** and **Cor-N1** peaking at -0.54 V and -0.58 V, respectively.

The properties of the three molecules for potential application in hydrogen evolution reaction (HER), oxygen evolution reaction (OER) and oxygen reduction reaction (ORR) have been investigated by tuning the solution conditions. The results for HER and OER of the molecules are shown in Figure 3 and that for ORR are displayed in Figure 4. Figure 3 shows linear sweep voltammetry (LSV) results of the electrodes fabricated with the three molecules in 0.5M H_2SO_4 solution. At a current density value of 10 mA·cm^{-2}, the potentials of **Cor-N1**, **Cor-N2** and **Cor-N3** are -0.374 V, -0.410 V and -0.393 V, respectively. The lowest potential is observed for **Cor-N1**, which indicates the best structure among the three for hydrogen evolution in acidic circumstance. Figure 3 shows LSV results of the electrodes fabricated with the three molecules in 0.1M NaOH solution. At a current density value of 10 mA·cm^{-2}, the potentials of **Cor-N1**, **Cor-N2** and **Cor-N3** are 1.924 V, 1.793 V and 1.882 V, respectively. The lowest potential is observed for **Cor-N2**, which indicates the best structure amongst the three for oxygen evolution in basic circumstance. By comparing the two cases in Figure 4, we find that the performance ability of the three molecules in terms of hydrogen evolution and oxygen evolution is in reverse sequence. For instance, **Cor-N2** is the worst in hydrogen evolution (Figure 3), while it attains the lowest potential for oxygen generation. **Cor-N3** shows the medium ability in both hydrogen and oxygen generation reactions. Figure 4 shows CV results of the electrodes fabricated with the three molecules in 0.5M H_2SO_4 and 0.1M NaOH solutions, respectively. Two oxidation and reduction peaks are observed in H_2SO_4 solution (Figure 4), indicating the two electron reaction processes for oxygen reduction. This may indicate that reduction of oxygen was first to an intermediate H_2O_2 at 0.4-0.45 V and then to H_2O at 0.7-0.75 V. Compared to the other counterparts, **Cor-N3** shows a clearer first reduction peak and the

lower potential of the second reduction reaction. A similar trend is observed for the three molecules when measuring the ORR under basic conditions (Figure 4). However, only one intense reduction peak is observed, suggesting that the reduction of oxygen follows a four-electron transfer pathway in strong base solution. Either the onset potential or the peak potential within the three molecules shows little or not clear variation, suggesting the change of numbers of nitrophenyl groups does not alter much on the ORR property. It is also worth to notice that **Cor-N2** shows promising ability in OER (Figure 3) but not the best choice for reduction reactions at the molecule/GO interface.

Conclusions

In summary, we have synthesized three cobalt(III) corrole molecules with different number of nitrophenyl groups at the periphery. Both structural and spectroscopic characterizations were performed and the compounds' electrocatalytic functions were tested and analysed in aqueous media considering their wide range of applications. **Cor-N1** performance is best for HER and **Cor-N2** is most suitable for OER. This behaviour signifies the effectiveness of these compounds to be applied in fuel cell developments.

Acknowledgements. This work was financially supported by the National Scientific Foundation of China (No. 21701058, 21771176) and the fund from Key Laboratory of Functional Inorganic Material Chemistry (Heilongjiang University), Ministry of Education.

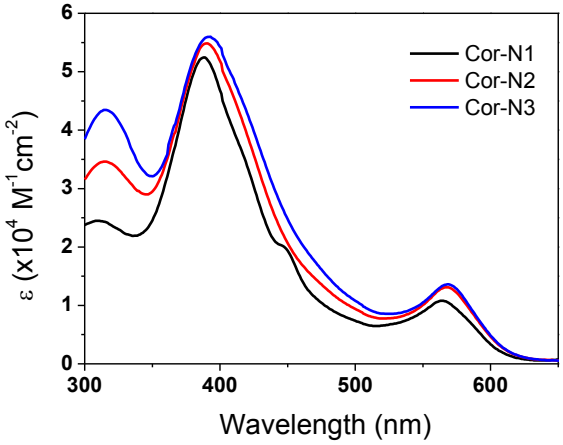

Figure 1. UV-visible absorption spectra of the investigated molecules **Cor-N1**, **Cor-N2** and **Cor-N3** in CH_2Cl_2

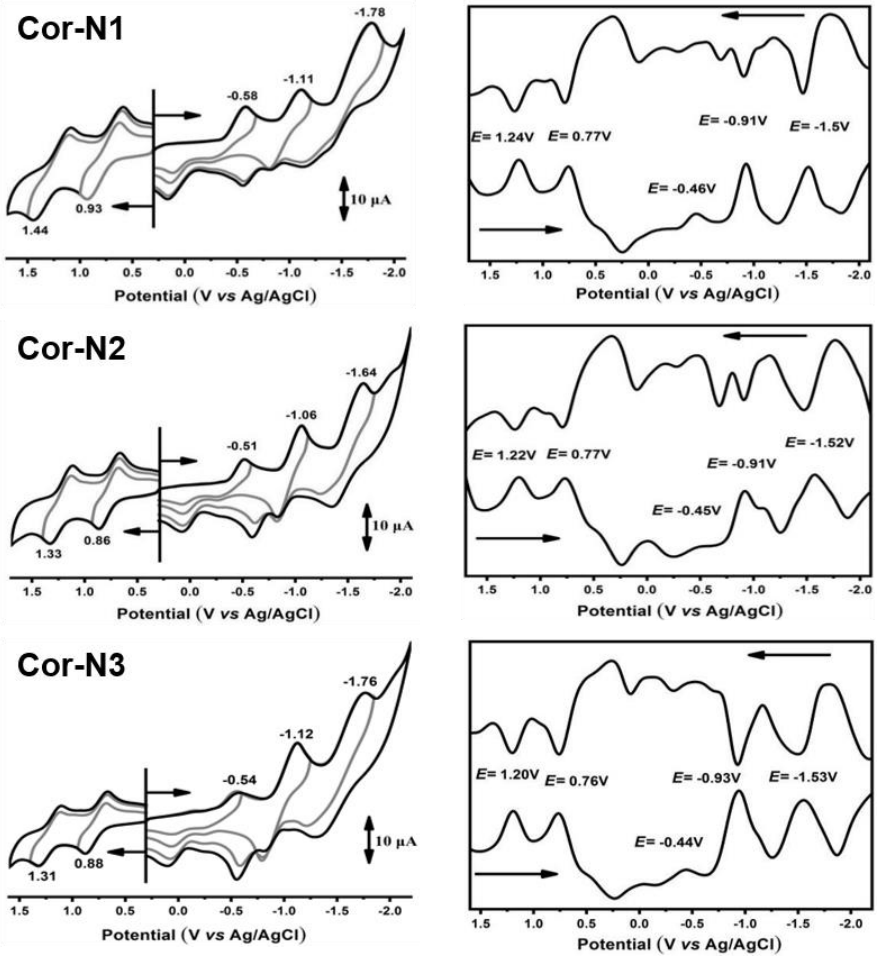

Figure 2. CV (left) and differential pulse voltammetry (DPV) (right) measurements of **Cor-N1**, **Cor-N2** and **Cor-N3** in *o*DCB containing 0.1 M TBAP.

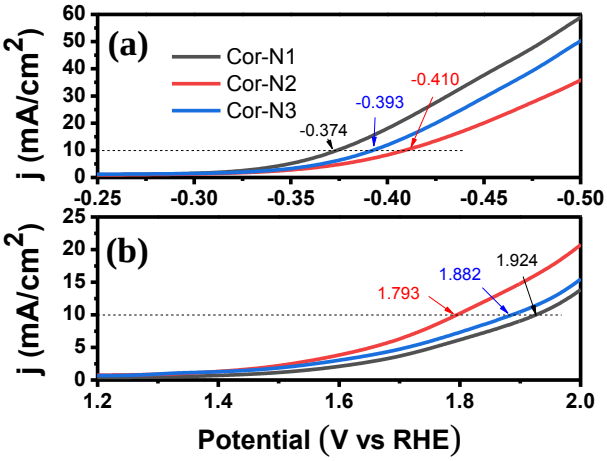

Figure 3. LSV measurements of rGO-supported **Cor-N1**, **Cor-N2** and **Cor-N3** in (a) 0.5M H_2SO_4 and (c) 0.1M NaOH under N_2.

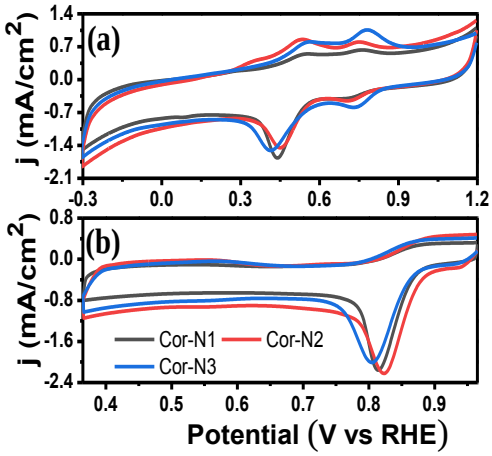

Figure 4. CV measurements of the investigated molecules on graphene oxide/GC electrode in (a) 0.5M H_2SO_4 and (b) 0.1M NaOH.

References

1. Zhang W., Lai W., Cao R. *Chem. Rev*. **2016**, *117*, 3717–3797.
2. Liang X., Qiu Y., Zhang X., Zhu W. *Dalton Trans*. **2020**, *49*, 3326–3332.
3. Zhao D., Zhuang Z., Cao X., Zhang C., Peng Q., Chen C., Li Y. *Chem. Soc. Rev*. **2020**, *49*, 2215–2264.
4. Pan Y., Sun K., Liu S., Cao X., Wu K., Cheong W.-C., Chen Z., Wang Y., Li Y., Liu Y. *J. Am. Chem. Soc.* **2018**, *140*, 2610–2618.
5. Attatsi I.K., Zhong H., Du J., Zhu W., Li M., Liang X. *Inorg. Chim. Acta* **2020**, *503*, 119398.
6. Nie Y., Li L., Wei Z. *Chem. Soc. Rev*. **2015**, *44*, 2168–2201.
7. Attatsi I.K., Zhu W., Liang X. *Inorg. Chim. Acta*. **2020**, *507*, 119584.
8. Wang N., Zheng H., Zhang W., Cao R. *Chin. J. Catal.* **2018**, *39*, 228–244.
9. Lin H., Hossain M.S., Zhan S.-Z., Liu H.-Y., Si L.-P. *Appl. Organomet. Chem*. **2020**, *34*, e5583.
10. Sahoo N.G., Pan Y., Li L., Chan S.H. *Adv. Mater*. **2012**, *24*, 4203–4210.
11. Faber M.S., Jin S. *Energy Env. Sci*. **2014**, *7*, 3519–3542.
12. Wang M., Chen L., Sun L. *Energy Environ. Sci.* **2012**, *5*, 6763–6778.
13. Galán- Mascarós J.R. *ChemElectroChem*. **2015**, *2*, 37–50.
14. Meng J., Lei H., Li X., Qi J., Zhang W., Cao R. *ACS Catal.* **2019**, *9*, 4551–4560.
15. Paolesse R., Mini S., Sagone F., Boschi T., Jaquinod L., Nurco D.J., Smith K.M. *Chem. Commun*. **1999**, 1307–1308.
16. Gross Z., Galili N., Saltsman I. *Angew. Chem. Int. Ed*. **1999**, *38*, 1427–1429.
17. Levy N., Mahammed A., Kosa M., Major D.T., Gross Z., Elbaz L. *Angew. Chem. Int. Ed*. **2015**, 54, 14080–14084.
18. Kumar A., Sujesh S., Varshney P., Paul A., Jeyaraman S. *Dalton Trans*. **2019**, *48*, 11345–11351.
19. Yuan H.-Q., Wang H.-H., Kandhadi J., Wang H., Zhan S.-Z., Liu H.-Y. *Appl. Organomet. Chem*. **2017**, *31*, e3773.
20. Mahammed A., Mondal B., Rana A., Dey A., Gros Z. *Chem Commun*. **2014**, *50*, 2725–2727.
21. Zhang X., Guo W., Zhu W., Liang X. *J. Porphyrins Phthalocyanines* **2021**, *25*, 273–281.
22. Xu L., Lei H., Zhang Z., Yao Z., Li J., Yu Z., Cao R. *Phys Chem Chem Phys* **2017**, *19*, 9755–9761.
23. Li X., Lei H., Guo X., Zhao X., Ding S., Gao X., Zhang W., Cao R. *ChemSusChem* **2017**, *10*, 4632–4641.
24. Zhang X., Wang Y., Zhu W., Mack J., Soy R.C., Nyokong T., Liang X. *Dyes Pigm*. **2020**, *175*, 108124.
25. Cummins D.C., Alvarado J.G., Zaragoza J.P.T., Effendy Mubarak M.Q., Lin Y.-T., de Visser S.P., Goldberg D.P. *Inorg. Chem*. **2020**, *59*, 16053–16064.
26. Zhang P., Li M., Jiang Y., Xu L., Liang X., Zhu W. *Macroheterocycles* **2015**, *8*, 65–70.
27. Du P., Eisenberg R. *Energy Environ. Sci*. **2012**, *5*, 6012–6021.
28. Dogutan D.K., McGuire R., Nocera D.G. *J. Am. Chem. Soc.* **2011**, *133*, 9178–9180.
29. Alemayehu A.B., Teat S.J., Borisov S.M., Ghosh A. *Inorg. Chem*. **2020**, *59*, 6382–6389.
30. Alemayehu A.B., McCormick-McPherson L.J., Conradie J., Ghosh A. *Inorg. Chem*. **2021**, *60*, 8315–8321.
31. Li M., Niu Y., Zhu W., Mack J., Fomo G., Nyokong T., Liang X. *Dyes Pigm*. **2017**, *137*, 523–531.
32. Nardis S., Mandoj F., Stefanelli M., Paolesse R. *Coord. Chem. Rev*. **2019**, *388*, 360–405.
33. Rongping Tang, Zhouqun Ji, Lin Xie, Hongyan Lu, Wei Tang, Xu Liang *Macroheterocycles* **2021**, *14*, 87–93.

Received 24.11.2021
Accepted 07.11.2022